British Journal of Pharmacology (2009), 156, 509–518

0007-1188/09
www.brjpharmacol.org

RESEARCH PAPER

Pharmacological characterization of recombinant NR1/NR2A NMDA receptors with truncated and deleted carboxy termini expressed in *Xenopus laevis* oocytes

CA Puddifoot[1], PE Chen[1], R Schoepfer[2] and DJA Wyllie[1]

[1]*Centres for Integrative Physiology and Neuroscience Research, University of Edinburgh, Edinburgh, UK, and* [2]*Department of Pharmacology, Laboratory for Molecular Pharmacology, University College London, London, UK*

Background and purpose: The carboxy terminal domain (CTD) of NR2 *N*-methyl-D-aspartate receptor (NMDAR) subunits interacts with numerous scaffolding and signal transduction proteins. Mutations of this region affect trafficking and downstream signalling of NMDARs. This study determines to what extent characteristic pharmacological properties of NR2A-containing NMDARs are influenced by this key functional domain.
Experimental approach: Using recombinant receptor expression in *Xenopus laevis* oocytes and two electrode voltage clamp recordings we characterized pharmacological properties of rat NR1/NR2A NMDARs with altered CTDs. We assessed the effects of truncating [at residue Iso1098; NR2A(trunC)] and deleting [from residue Phe822; NR2A(delC)] the CTD of NR2A NMDAR subunits on agonist potencies, channel block by Mg^{2+} and memantine and potentiation of NMDAR-mediated responses by chelating contaminating divalent cations.
Key results: Truncation or deletion of the CTD of NR2A NMDAR subunits did not affect glutamate potency [EC_{50} = 2.2 μmol·L^{-1}, NR2A(trunC); 2.7 μmol·L^{-1}, NR2A(delC) compared with 3.3 μmol·L^{-1}, NR2A(WT)] but did significantly increase glycine potency [EC_{50} = 500 nmol·L^{-1}, NR2A(trunC); 900 nmol·L^{-1}, NR2A(delC) compared with 1.3 μmol·L^{-1}, NR2A(WT)]. Voltage-dependent Mg^{2+} block of NR2A(WT)- and NR2A(trunC)-containing NMDARs was similar but low concentrations of Mg^{2+} (1 μmol·L^{-1}) potentiated NR1/NR2A(delC) NMDARs. Memantine block was not affected by changes to the structure of the NR2A CTD. EDTA-induced potentiation was similar at each of the three NMDAR constructs.
Conclusions and implications: Of the parameters studied only minor influences of the CTD were observed; these are unlikely to compromise interpretation of studies that make use of CTD-mutated recombinant receptors or transgenic mice in investigations of the role of the CTD in NMDAR signalling.
British Journal of Pharmacology (2009) **156**, 509–518; doi:10.1111/j.1476-5381.2008.00040.x; published online 19 January 2009

Keywords: NMDA; glutamate; glycine; memantine; oocyte; two electrode voltage clamp; electrophysiology; ion channel

Abbreviations: ATD, amino terminal domain; CTD, carboxy terminal domain; LBD, ligand binding domain; NMDAR, *N*-methyl-D-aspartate receptor; TEVC, two electrode voltage clamp

Introduction

N-methyl-D-aspartate receptors (NMDARs) are subtypes of ionotropic glutamate receptors expressed abundantly throughout the central nervous system. These heterotetrameric proteins are thought to form a dimer-of-dimers assembly (Furukawa *et al.*, 2005) of two glycine-binding NR1 subunits and two glutamate-binding NR2 subunits (reviewed in Chen and Wyllie, 2006). In addition to ligand binding, NMDARs require the relief of a voltage-dependent block by extracellular Mg^{2+} for ion permeation through the channel pore to occur. Combined with its high permeability to Ca^{2+}, these properties have implicated NMDARs in a number of inter- and intra-cellular processes such as synaptogenesis, pro-death and pro-survival signalling and long-term potentiation in addition to their primary role in 'fast' glutamatergic synaptic transmission (Dingledine *et al.*, 1999).

The NR1 subunits are encoded by one gene (which generates eight splice variants) while NR2 subunits are encoded by

Correspondence: Dr David J.A. Wyllie, Centres for Integrative Physiology and Neuroscience Research, Hugh Robson Building, University of Edinburgh, George Square, Edinburgh EH8 9XD, UK. E-mail: dwyllie1@staffmail.ed.ac.uk
Received 23 June 2008; revised 23 September 2008; accepted 29 September 2008

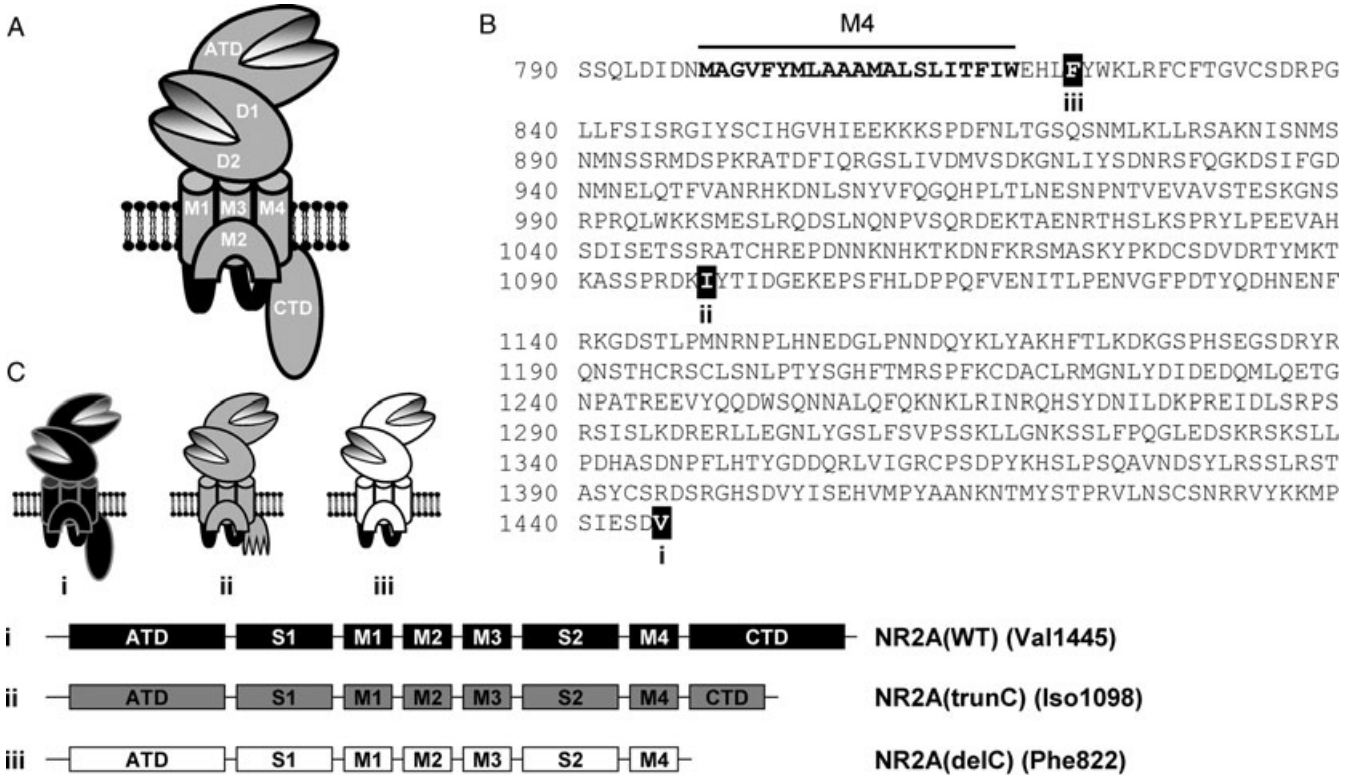

Figure 1 Representation of the NR2A NMDAR subunits used in this study. (A) Cartoon representation of an NMDAR subunit showing the proposed membrane topology of three membrane spanning domains (M1, M3 and M4) and a re-entrant loop (M2) and the location of the amino terminal domain (ATD) and carboxy terminal domain (CTD). The ligand binding domains (denoted D1 and D2) are formed by the S1 and S2 regions of the protein which come together to form a hinged clamshell-like structure. (B) Amino acid sequence of part of the NR2A NMDAR subunit. The letters shown in bold indicate the M4 region while each of the residues labelled as i, ii and iii indicate the last amino acid contained within each of the subunits studied. The full-length NR2A(WT) subunit contains 1145 residues and ends at Val1445 (i); the NR2A(trunC) NMDAR subunit ends at Iso1098 (ii) while the NR2A(delC) NMDAR subunit contains only four residues of the carboxy terminal and ends at Phe822 (iii). (C) Cartoon depiction and linear representation of the structure of each of the three NR2A NMDAR subunits investigated in this study.

four different genes giving rise to four distinct subunits A–D (Monyer *et al.*, 1992). The NR2 subtype contained within any given receptor defines the majority of its biophysical and pharmacological properties (Monyer *et al.*, 1994; reviewed in Cull-Candy *et al.*, 2001; Erreger *et al.*, 2004). Both NR1 and NR2 possess four well-defined functional domains (see Figure 1a). These are an extracellular amino terminal domain (ATD) and ligand binding domain (LBD) formed by regions D1 and D2, three membrane spanning domains (M1, M3 and M4) together with a re-entrant loop (M2) which form the channel pore and an intracellularly located carboxy terminal domain (CTD) which interacts with numerous membrane scaffolding and signalling proteins. The contribution of the ligand binding and membrane spanning domains to the functional properties of the receptor was recently investigated using chimeric NR2 constructs (Chen *et al.*, 2008; Wrighton *et al.*, 2008) which showed that regions outwith those normally associated with particular functions could influence agonist potency and ion permeation. For example, the LBD can influence the potency of voltage-dependent Mg^{2+} block (Wrighton *et al.*, 2008) and protein–protein interactions at the interface of NR1 and NR2 NMDAR subunits determine aspects of channel gating (Chen *et al.*, 2008). This suggests the functional domains of NMDAR subunits have more widespread influences on receptor-channel function and that it was of merit to investigate whether the intracellularly located CTD of NR2A subunits played a role in either determining agonist potency at, or influencing voltage-dependent Mg^{2+} block of NMDARs

Previous studies into the role of the CTD in physiology and pathology of neurons have shown that either disrupting the NR2A CTD interactions with intracellular proteins of the postsynaptic density or truncating the CTD alters a number of cellular functions. These include synaptogenesis and trafficking of new NMDARs to synapses (Steigerwald *et al.*, 2000; Rossi *et al.*, 2002) associated with learning and memory (Migaud *et al.*, 1998; Sprengel *et al.*, 1998), and pathological processes involved in excitotoxicity and chronic pain (Garry *et al.*, 2003). Nevertheless, basic pharmacological characterization of NMDARs containing NR2A subunits with altered carboxy termini is lacking. Moreover, a number of previous studies have suggested that the CTD may influence agonist sensitivity in recombinant NMDARs through the interactions of CTD associated intracellular signalling proteins such as the PDZ-containing proteins, PSD-95 and MALS-2 (Yamada *et al.*, 1999; Rutter and Stephenson 2000; Rutter *et al.*, 2002; Iwamoto *et al.*, 2004). Although the extent to which endogenous scaffolding proteins for the NMDAR subunits are

present in recombinant expression systems remains to be established, a number of studies have used *Xenopus* oocytes to assess the effect of recombinantly expressed cytoskeletal proteins on NMDAR function (Yamada *et al.*, 1999; Iwamoto *et al.*, 2004; Lin *et al.*, 2004; 2006). Thus, by studying NMDAR pharmacology in a recombinant system, where the signalling and scaffolding proteins that the CTD normally interacts with are most likely absent, it is possible to determine what additional functional roles this domain might play in basic NMDAR pharmacology.

Methods

Plasmid constructs, cRNA synthesis and receptor expression in oocytes

The pSP64T-derived expression plasmids for rat NR1-1a (excluding exon 5, including exons 21 and 22, which we will refer to as 'NR1') and wild-type NR2A NMDA receptor subunits have been described previously (Chen *et al.*, 2005). Truncated and deleted NR2A NMDAR subunits constructs were generated from wild-type NR2A cDNAs with cleavage sites at Isoleucine 1098 and Phenylalanine 822, respectively, as depicted in Figure 1B. We refer to these subunits as NR2A(trunC) and NR2A(delC). The NR2A(trunC) subunit lacks the sequence motifs for a number of cytoskeletal proteins that are known to associate with the NR2 subunit (e.g. PSD-95 and CaMKII) (Kornau *et al.*, 1995; Gardoni *et al.*, 2001; Ryan *et al.*, 2008) while the NR2A(delC) construct contains only four amino acid residues C-terminal of the M4 region. Each of these NR2A C-terminal mutants contains the three amino acid residues (FHL) located immediately after M4 which are necessary for export from the endoplasm (Hawkins *et al.*, 2004). Cartoon depictions of these together with wild-type NR2A NMDAR subunits are illustrated in Figure 1C. cRNA was synthesized as runoff transcripts from Mlu I linearized plasmid DNA using the SP6 polymerase RiboMax RNA synthesis kit. Reactions were supplemented with 0.75 mmol·L^{-1} capping nucleotide, m^{7}G(5′)ppp(5′)G in the presence of 1.6 mmol·L^{-1} GTP. Integrity and yield of each synthesized cRNA was verified by fluorescence intensity in ethidium bromide-stained agarose gels. For recombinant NMDA receptor expression, NR1 and one of either the NR2A(WT), NR2A(trunC) or NR2A(delC) cRNAs were mixed at a nominal ratio of 1:1 and diluted with nuclease-free water to 5 ng·μL^{-1}, prior to injection. The NMDAR subunits which we refer to as 'NR1' and 'NR2A' are now recommended by the NC-IUPHAR to be called GluN1, GluN2A and GluN2B, respectively (see Alexander *et al.*, 2008), but for consistency with our previous publications we shall continue to use the older nomenclature in this study.

Stage V–VI oocytes were obtained from *Xenopus laevis* that had been anaesthetized by immersion in a solution of 3-amino-benzoic acid ethylester (0.5%) and then killed by injection of an overdose solution of pentobarbital (0.4 mL of 20% solution) followed by decapitation and exsanguation after the confirmation of loss of cardiac output. All procedures were carried out in accordance with current UK Home Office. Prior to injection with cRNA mixtures of interest, the follicular membranes of the oocytes were removed. After injection oocytes were placed in separate wells of 24-well plates containing a modified Barth's solution with composition (in mmol·L^{-1}): NaCl 88, KCl 1, $NaHCO_3$ 2.4, $MgCl_2$ 0.82, $CaCl_2$ 0.77, Tris-Cl 15, adjusted to pH 7.35 with NaOH. This solution was supplemented with 50 IU·mL^{-1} penicillin and 50 μg·mL^{-1} streptomycin. Oocytes were placed in an incubator (19°C) for 24–48 h to allow for receptor expression and then stored at 4°C until required for electrophysiological measurements.

Electrophysiological recordings and solutions

Two electrode voltage clamp (TEVC) recordings were made using a GeneClamp 500 from oocytes that were placed in a solution that contained (in mmol·L^{-1}): NaCl 115, KCl 2.5, HEPES 10, $BaCl_2$ 1.8, EDTA 0.01; pH 7.3 with NaOH (20°C). EDTA (10 μmol·L^{-1}) was added to chelate contaminant extracellular divalent ions, including trace amounts of Zn^{2+}. Current and voltage electrodes were made from thin-walled borosilicate glass using a PP-830 electrode puller and when filled with 3 mol·L^{-1} KCl possessed resistances of between 0.5 and 1.5 MΩ. Oocytes were voltage-clamped at –40, –60 or –80 mV. For L-glutamate concentration-response measurements, the recording solution was further supplemented with glycine (50 μmol·L^{-1}) and for glycine dose-response measurements this solution was supplemented with glutamate (100 μmol·L^{-1}). Application of solutions was controlled manually and data were filtered at 10 Hz and digitized at 100 Hz via a Digidata 1200 A/D interface using WinEDR software. Test solutions were applied for 20–60 s or until a plateau to the agonist-evoked response had been achieved. NR2A(WT)-, NR2A(trunC)- and NR2A(delC)-containing NMDARs gave similar levels of expression as judged by the range of current amplitudes recorded.

Agonist concentration-response curves

For agonist concentration-response curves glutamate or glycine (0.1–300 μmol·L^{-1}) were applied cumulatively on a background of a saturating solution of glycine (50 μmol·L^{-1}) or glutamate (100 μmol·L^{-1}), respectively, and agonist-evoked currents recorded. Individual concentration-response curves were fitted with the Hill equation:

$$I = I_{max} / \left(1 + ([A]/EC_{50})^{nH}\right),$$

where I = current response to agonist concentration [A], I_{max} = predicted maximum response, EC_{50} = concentration of agonist that gives a half-maximal response and n_H = Hill coefficient. To give an overall mean EC_{50} value, data points were normalized to the predicted maximum, pooled and re-fitted with the Hill equation, with the maximum and minimum for each curve being constrained to asymptote to 1 and 0, respectively (see Frizelle *et al.*, 2006; Wyllie and Chen, 2007)

Mg^{2+}, memantine and Zn^{2+} inhibition

Inhibition by Mg^{2+} and memantine was expressed as a percentage inhibition of the glutamate/glycine-evoked current recorded in the absence of these channel blockers. To estimate the extent of inhibition caused by contaminant levels of Zn^{2+} in the external solution, glutamate/glycine-evoked currents

were recorded in an external solution containing a lower concentration of $BaCl_2$ (0.18 mmol·L^{-1}); this solution contained no EDTA. Once a steady-state response was achieved a solution containing EDTA (10 μmol·L^{-1}) was added and the increase in the current expressed as a percentage of the current initially recorded.

Materials

SP6 polymerase RiboMax RNA synthesis kit and $m^7G(5')ppp(5')G$ were obtained from Promega (Madison, WI, USA); penicillin and streptomycin, Invitrogen (Paisley, UK). The GeneClamp 500 was from Molecular Devices (Union City, CA, USA); the thin-walled borosilicate glass (GC150TF-7.5) was from Harvard Apparatus (Kent, UK) and the PP-830 electrode puller from Narashige Instruments (Japan). The Digidata 1200 was from Molecular Devices (Union City, CA, USA) and WinEDR software was Strathclyde Electrophysiology Software (Strathclyde University, UK). All chemicals were purchased from Sigma-Aldrich (Poole, UK) with the exception of the memantine (Tocris Bioscience, Bristol, UK).

Statistical analysis

Results are presented as mean ± SEM and statistical comparison between data sets was assessed using either Student's *t*-test (paired where appropriate) or two-way ANOVA tests (GraphPad Prism v5.0) to determine whether differences were significant ($P < 0.05$). Microcal Origin v6.0 software was used for graphical presentation.

Results

Concentration-response curves for NR1/NR2A(trunC) and NR1/NR2A(delC) NMDARs

We assessed first whether truncating or deleting the carboxy terminal of NR2A NMDAR subunits affected the potency of either glutamate or glycine. Figure 2A shows a typical TEVC current recording from an oocyte expressing NR1/NR2A(delC) NMDARs where cumulative increases in the concentration of glutamate (in the presence of glycine, 50 μmol·L^{-1}) were applied to determine its EC_{50}. Mean glutamate concentration-response curves obtained for NR1/NR2A(trunC) and NR1/NR2A(delC) NMDARs are illustrated in Figure 2B,C and gave mean EC_{50} values of 2.2 ± 0.2 μmol·L^{-1} ($n = 8$) and 2.7 ± 0.3 μmol·L^{-1} ($n = 10$) respectively. These values are not significantly different for those we obtained previously for glutamate acting at NR1/NR2A NMDARs (Chen *et al.*, 2005; 2008; Erreger *et al.*, 2007). Figure 2D shows a typical TEVC current recording from an oocyte expressing NR1/NR2A(delC) NMDARs where cumulative increases in the concentration of glycine, on a background of glutamate (100 μmol·L^{-1}), were applied to determine its EC_{50}. The mean EC_{50} values for glycine (Figure 2E,F) acting at NR2A(trunC)- and NR2A(delC)-containing NMDARs were 0.50 ± 0.1 μmol·L^{-1} ($n = 6$) and 0.9 ± 0.1 μmol·L^{-1} ($n = 6$) respectively. Thus, glycine displays significantly ($P < 0.05$) higher potency at both of these NR2A constructs compared with NR2A(WT)-containing NMDARs (EC_{50} = 1.3 μmol·L^{-1}; Chen *et al.*, 2008). In each of the panels the dashed line shows data obtained previously (Erreger *et al.*, 2007; Chen *et al.*, 2008) for concentration-response curves for both agonists recorded under similar recording conditions but acting at NR1/NR2A(WT) NMDARs.

Mg^{2+} and memantine block of NR1/NR2A(WT), NR1/NR2A(trunC) and NR1/NR2A(delC) NMDARs

NMDARs are blocked in a voltage-dependent manner by Mg^{2+} (Mayer *et al.*, 1984; Nowak *et al.*, 1984). While the major determinants of the properties of this block reside in the M2 region of NMDAR subunits, in particular the QRN site (Burnashev *et al.* 1992) and the N_{+1} site (Wollmuth *et al.* 1998), other parts of the protein outwith the pore-forming regions contribute to the potency of Mg^{2+} block (e.g. see Kuner and Schoepfer, 1996; Wrighton *et al.*, 2008). No studies to date have quantified the effect of removing the carboxy terminal on this characteristic property of NMDARs. Figure 3 shows the effects of Mg^{2+} (1 μmol·L^{-1}–1 mmol·L^{-1}) on glutamate/glycine-evoked currents at each of the three constructs investigated in this study. For NR1/NR2A(WT) (Figure 3A) and NR1/NR2A(trunC) (Figure 3B) NMDARs, typical voltage-dependent inhibition by Mg^{2+} was observed. The extent of the inhibition at each of the potentials examined was similar to that recently reported (Wrighton *et al.*, 2008) and no significant differences in Mg^{2+} block between NR1/NR2A(WT) and NR1/NR2A(trunC) NMDARs were observed (Figure 3D–F; $P > 0.05$, one-way ANOVA). For NR1/NR2A(delC) NMDARs, however, we consistently observed potentiation of glutamate/glycine-evoked currents in the presence of low (1 μmol·L^{-1}) concentrations of Mg^{2+}. The TEVC trace in Figure 3C shows a typical recording from an oocyte expressing NR1/NR2A(delC) NMDARs recorded at a holding potential of –40 mV. The mean potentiation observed at –40 mV with Mg^{2+} (1 μmol·L^{-1}) was 17 ± 5% ($n = 8$). Indeed at this depolarized holding potential net potentiation was observed with both 1 and 10 μmol·L^{-1} Mg^{2+}. For the lowest Mg^{2+} concentration used, we also observed potentiation at –60 and –80 mV (Figure 3D–F). At higher concentrations Mg^{2+} (100 μmol·L^{-1} and 1 mmol·L^{-1}) blocked NR1/NR2A(delC) NMDARs to a similar extent to that seen for NR1/NR2A(WT) and NR1/NR2A(trunC) NMDARs.

We were intrigued to assess whether the potentiation of NR1/NR2A(delC) NMDAR-mediated currents extended to other channel blockers. Memantine is a potent blocker of NMDAR-mediated responses (Parsons *et al.*, 1999; Chen and Lipton, 2005; Dravid *et al.*, 2007; Wrighton *et al.*, 2008) binding to both low and high affinity sites within the channel pore; the asparagine residue of the QRN site being a major determinant of the latter of these two sites. Figure 4A–C shows typical TEVC traces for each of the NMDAR constructs and the effects of memantine (0.1–30 μmol·L^{-1}) on the glutamate/glycine-evoked currents. Quantification of the extent of the memantine block (Figure 4D–F) reveals, and in contrast to Mg^{2+} block, that there were no differences in the magnitude of the memantine block at any of the concentrations or the holding potentials examined.

EDTA potentiation of NR1/NR2A(WT), NR1/NR2A(trunC) and NR1/NR2A(delC) NMDARs

NR2A-containing NMDARs are inhibited by low (<100 nmol·L^{-1}) extracellular concentrations of Zn^{2+} (Paoletti

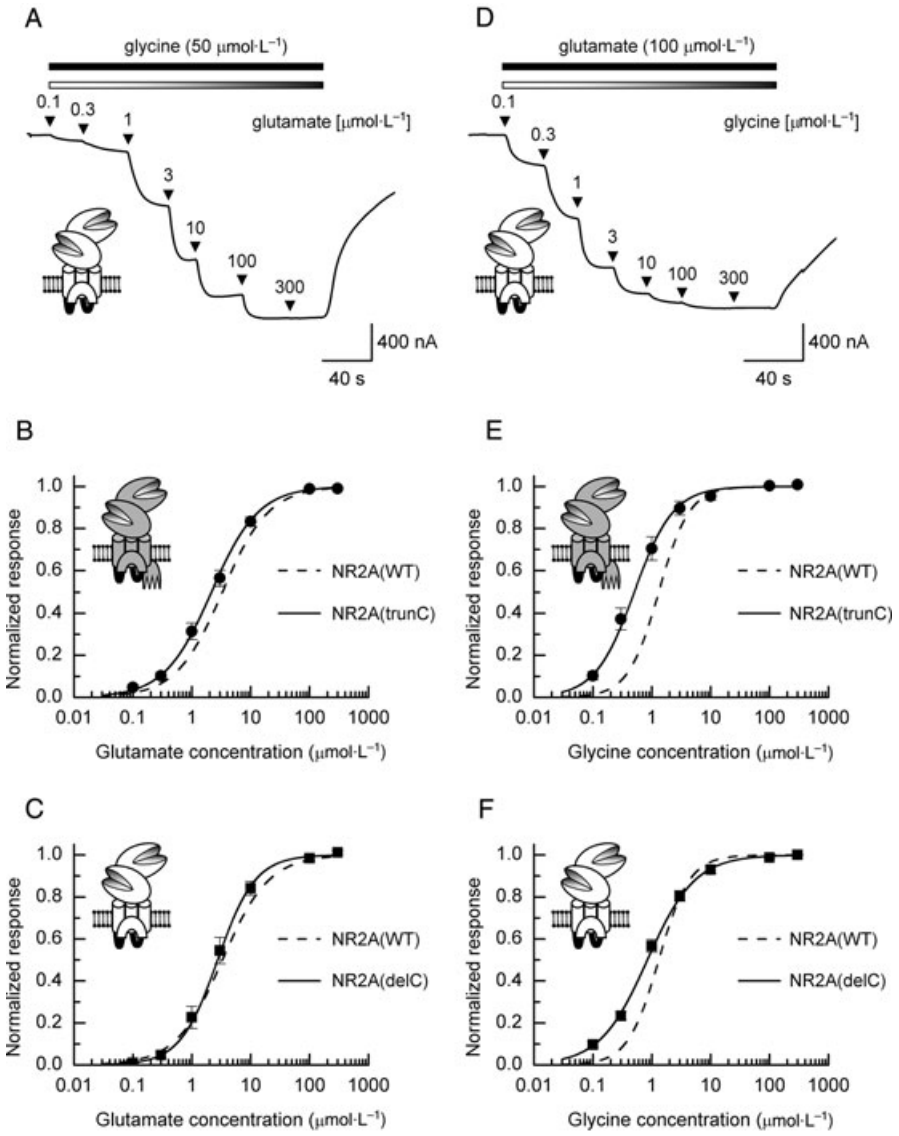

Figure 2 Concentration-response curves for NR1/NR2A(trunC) and NR1/NR2A(delC) NMDARs. (A) Example of a TEVC current recording obtained from an oocyte expressing NR1/NR2A(delC) NMDARs. In the presence of glycine (50 μmol·L^{-1}), increasing concentrations of glutamate (100 nmol·L^{-1}–300 μmol·L^{-1}) were applied cumulatively. (B) Mean concentration-response curve for glutamate-evoked currents recorded from oocytes expressing NR1/NR2A(trunC) NMDARs. The data points are fitted with the Hill equation, which gives an EC_{50} value of 2.5 μmol·L^{-1} ($n = 8$). (C) Mean concentration-response curve for glutamate-evoked currents recorded from oocytes expressing NR1/NR2A(delC) NMDARs, the EC_{50} is 3.2 μmol·L^{-1} ($n = 12$). (D) As in (A) but showing a TEVC current trace obtained in the presence of glutamate (100 μmol·L^{-1}) and the cumulative addition of increasing concentrations of glycine (100 nmol·L^{-1}–300 μmol·L^{-1}). (E) Mean concentration-response curve for glycine acting at NR1/NR2A(trunC) NMDARs, the estimated EC_{50} value is 0.46 μmol·L^{-1} ($n = 6$). (F) Mean concentration-response curve for glycine-evoked currents recorded from oocytes expressing NR1/NR2(delC) NMDARs, the EC_{50} is 1.4 μmol·L^{-1} ($n = 6$). The mean maximal currents recorded for glutamate concentration-response curves were 3.1 ± 1.0 μA and 7.9 ± 0.7 μA and for glycine concentration-response curves were 5.0 ± 0.7 μA and 5.1 ± 0.7 μA for oocytes expressing NR1/NR2A(trunC) and NR1/NR2A(delC) NMDARs respectively. The dashed lines in each of the panels indicate the mean concentration-response curves for glutamate or glycine acting at NR1/NR2A(WT) NMDARs. Data originally presented in Erreger *et al.* (2007) for (B) and (C) and in Chen *et al.* (2008) for (E) and (F).

et al., 1997; Traynelis *et al.*, 1998). This high affinity site for Zn^{2+} is located in the ATD and sufficient levels of Zn^{2+} are found as a 'contaminant' in the external solution used for electrophysiological recordings to result in a significant inhibition of NR2A-containing NMDARs. Indeed for this reason we added EDTA (10 μmol·L^{-1}) to chelate this and other divalent cations. The voltage-independent block by low concentrations of Zn^{2+} can be reduced by the actions of Src, a tyrosine kinase (Zheng *et al.*, 1998). Moreover, point mutation of any of three tyrosine residues, Y1086, Y1248 and Y1368 (numbering as used in Figure 1B) prevents the ability of Src to potentiate NR1/NR2A NMDAR-mediated currents. These data suggest that interactions between the intracellular CTD and extracellular ATD exist. We therefore considered whether mutations to the CTD would manifest themselves as a change in the receptor's sensitivity to these low levels of contaminating Zn^{2+}. Figure 5A–C shows typical TEVC traces recorded from oocytes expressing NR1/NR2A(WT), NR1/NR2A(trunC)

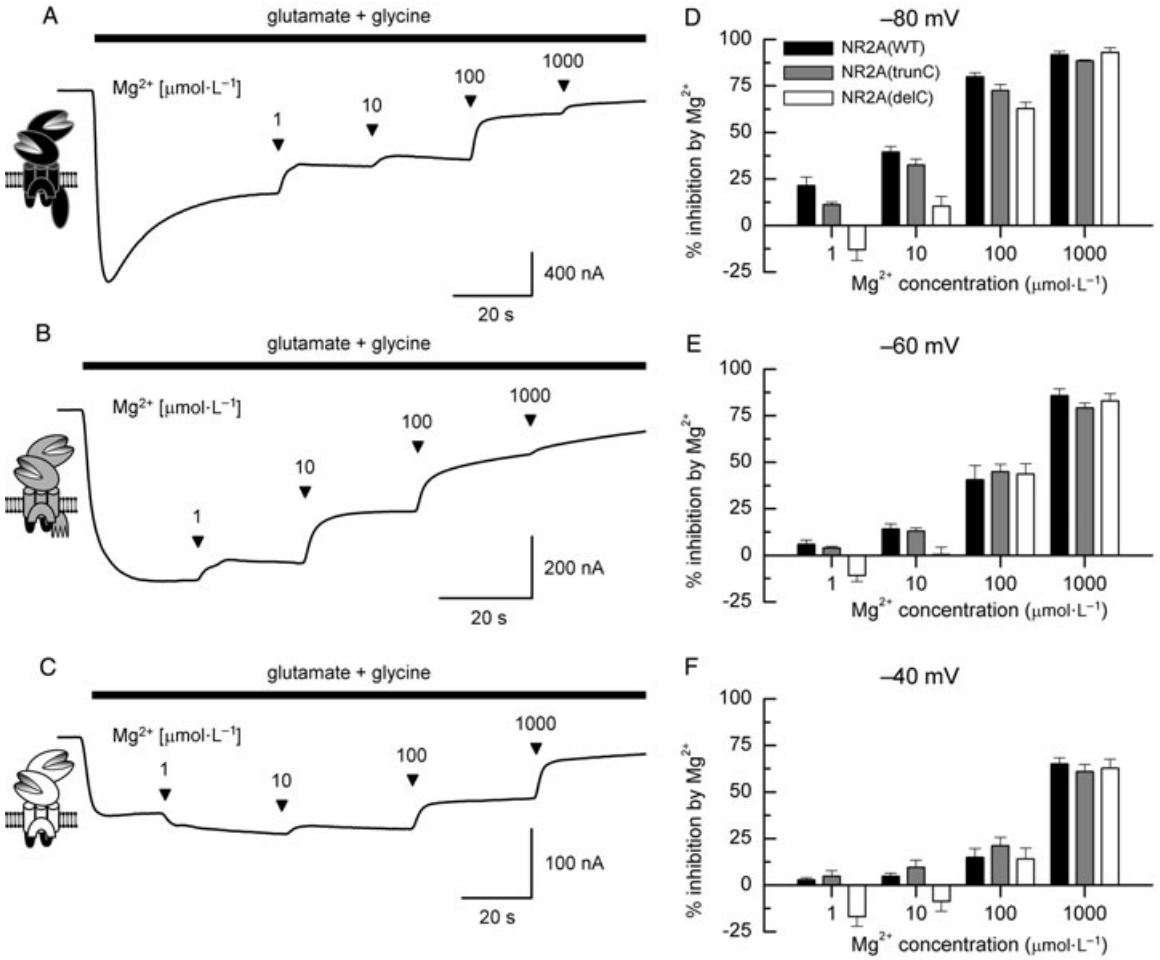

Figure 3 Mg^{2+} inhibition of NR1/NR2A(WT), NR1/NR2A(trunC) and NR1/NR2A(delC) NMDARs. (A) TEVC current trace, at –80 mV, of glutamate-evoked current recorded from an oocyte expressing NR1/NR2A(WT) NMDARs. NMDAR-mediated currents are shown in the absence (control) and presence of increasing concentrations of Mg^{2+} (1 μmol·L^{-1}–1 mmol·L^{-1}). (B) As (A) but obtained from an oocyte expressing NR1/NR2A(trunC) NMDARs. (C) TEVC trace, recorded at –40 mV, illustrating the novel finding of Mg^{2+}-induced potentiation, at low Mg^{2+} concentrations, of NR1/NR2A(delC) NMDAR-mediated currents. (D–F) Histograms showing the mean percentage inhibition of glutamate-evoked currents by Mg^{2+} for oocytes voltage-clamped at –80, –60 and –40 mV.

and NR1/NR2A(delC) NMDARs respectively. Following the application of a saturating glutamate/glycine-containing solution and the establishment of a steady-state response, the solution was switched to one containing EDTA (10 μmol·L^{-1}). Currents recorded from each of the NMDAR constructs showed potentiation. The quantification of this potentiation is illustrated in Figure 5D. Mean potentiation for NR1/NR2A(WT), NR1/NR2A(trunC) and NR1/NR2A(delC) NMDARs was 29 ± 4% ($n = 8$), 23 ± 3% ($n = 7$) and 29 ± 9% ($n = 9$) respectively. These values are not significantly different ($P > 0.05$; one-way ANOVA).

Discussion

The aim of this study was to assess the contribution of the CTD of the NR2A subunit to basic pharmacological properties of NMDARs. While the CTD comprises around a third of the total NR2A NMDAR subunit and plays a pivotal role in interacting with scaffolding proteins and the NMDAR signalling complex, it is not required for functional channel expression, as assayed in our recombinant expression system. Moreover, examination of the CTD amino acid residues from the four different NR2 subunits reveals a lower degree of sequence identity than the highly conserved amino terminal and membrane spanning regions (Ryan *et al.*, 2008). Previous studies have shown, however, that mice expressing NR2A NMDARs lacking their CTDs while still being able to participate in synaptic transmission (albeit at lower expression levels), display impaired contextual memory and reduced long-term potentiation (Sprengel *et al.*, 1998). Furthermore, mice expressing NR2A and NR2C NMDAR subunits each with truncated CTDs give rise to NMDARs with impaired activation and reduced open probability (Rossi *et al.*, 2002). This latter study indicates that the intracellularly located CTD may interact with other regions of the NMDAR controlling its activation properties and highlights the importance of inter-domain interactions in controlling NMDAR function (see also Chen *et al.*, 2008; Wrighton *et al.*, 2008). The use of recombinant expression systems to study NMDAR function allows us to

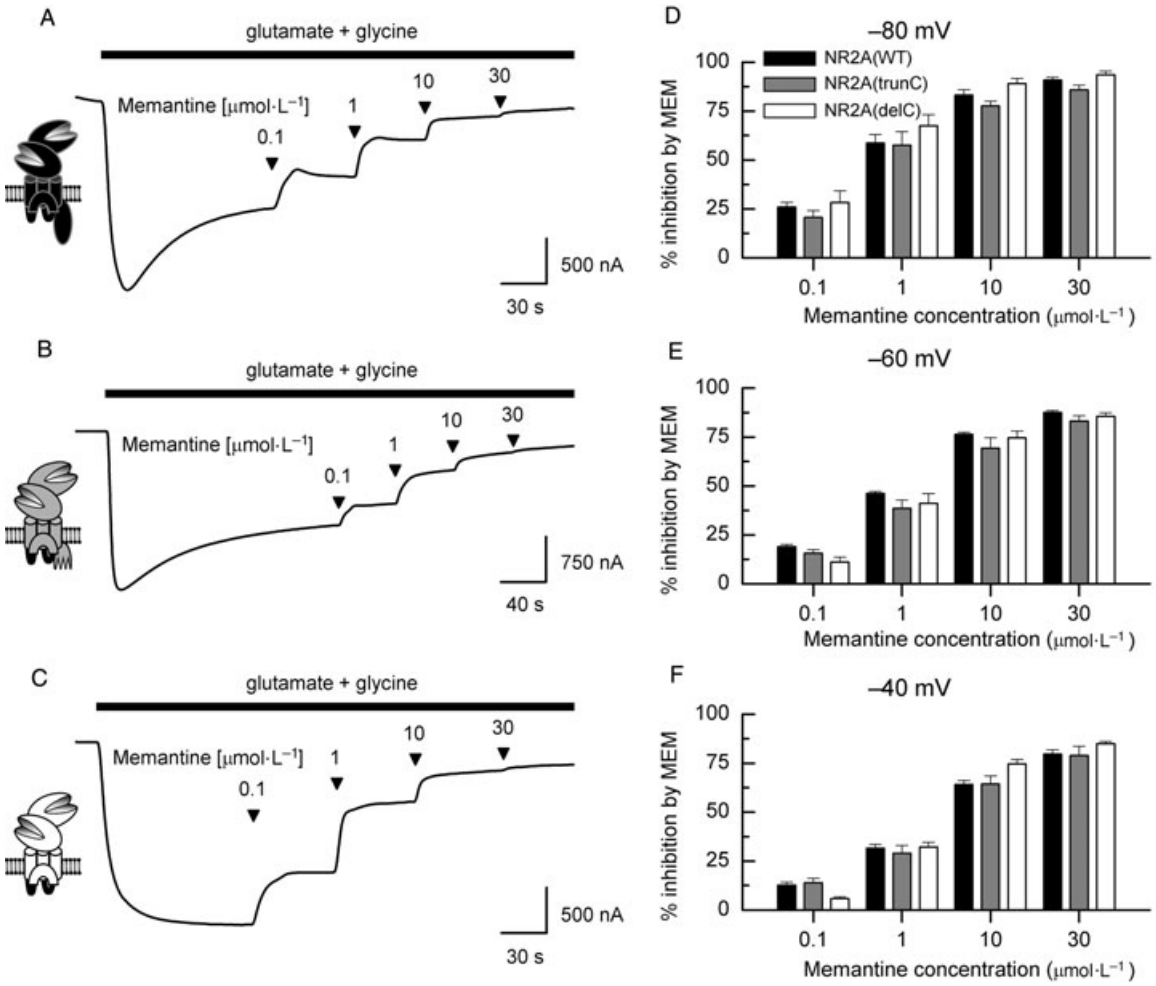

Figure 4 Memantine inhibition of NR1/NR2A(WT), NR1/NR2A(trunC) and NR1/NR2A(delC) NMDARs. (A) TEVC current trace, at –80 mV, of glutamate-evoked current recorded from an oocyte expressing NR1/NR2A(WT) NMDARs. NMDAR-mediated currents are shown in the absence (control) and presence of increasing concentrations of memantine (0.1–30 μmol·L^{-1}). (B and C) As in (A) but obtained from oocytes expressing NR1/NR2A(trunC) NMDARs (B) or NR1/NR2A(delC) NMDARs (C). (D–F) Histograms showing the mean percentage inhibition of glutamate-evoked currents by memantine for oocytes voltage-clamped at –80, –60 and –40 mV.

identify clearly how these 'functional' domains may influence NMDAR properties. In such systems, however, we do not know to what extent endogenous proteins interact with the recombinant protein to alter its activity.

Glutamate potency was not affected by truncation or deletion of the CTD whereas for both NR2A(trunC)- and NR2A(delC)-containing NMDARs we observed a significant increase in the potency of the co-agonist, glycine. We have recently described the ability of the NR2 LBD to influence glycine potency (Chen *et al.*, 2008). The effect appears to be due to protein–protein interactions between residues outwith the binding pocket but located in the S2 region of the NR2 NMDAR subunits and residues in the S2 region of the NR1 NMDAR subunit. The data presented here add to the notion of protein–protein interactions between NR1 and NR2 NMDAR subunits; however, further investigation is required to determine whether this modulation of glycine potency is brought about simply because of aberrant assembly/altered protein folding of the NMDAR complex due to the loss of the NR2A CTD or loss of specific CTD interactions between NR1 and NR2 NMDAR subunits. An intriguing observation in our characterization of CTD-mutant NR1/NR2A NMDARs was the finding that low extracellular Mg^{2+} concentrations (1 μmol·L^{-1}) caused a small potentiation of NR1/NR2A(delC) NMDAR-mediated responses. This potentiating action of Mg^{2+} was voltage-independent. However, at higher concentrations of Mg^{2+} (100 μmol·L^{-1} or 1 mmol·L^{-1}) a characteristic voltage-dependent block was observed that was not different from that seen for either NR2/NR2A(trunC) or NR1/NR2A(WT) NMDARs. Potentiation of NMDAR-mediated currents has been reported previously. Extracellular Mg^{2+} can potentiate NR1/NR2B (but not NR1/NR2A) NMDAR-mediated currents (Paoletti *et al.*, 1995; also see Wang and MacDonald, 1995). However, the potentiation at NR2B-containing NMDARs is greater than we observed here for potentiation of NR1/NR2A(delC) NMDARs, is seen with millimolar concentrations of Mg^{2+} and occurs at positive potentials where voltage-dependent block is absent. This NR2B-dependent potentiation is thought to result from an interaction of Mg^{2+}

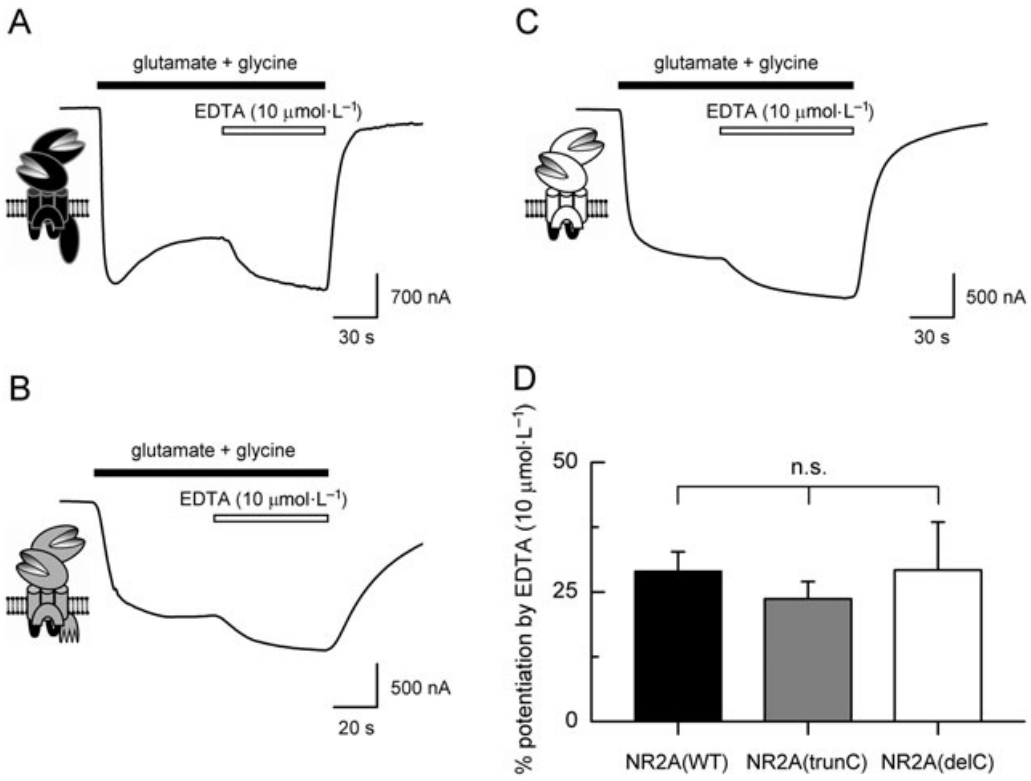

Figure 5 EDTA-induced potentiation of NR1/NR2A(WT), NR1/NR2A(trunC) and NR1/NR2A(delC) NMDARs. (A) TEVC current trace, at –40 mV, of glutamate-evoked current recorded in a low $BaCl_2$ (0.18 mmol·L^{-1}) external solution. Once a steady-steady response was obtained, the solution was switched to one containing EDTA (10 μmol·L^{-1}). This resulted in an increase in the level of current recorded due to the chelation of contaminant levels of certain divalent cations (mainly Zn^{2+}). (B and C) As (A) but illustrating TEVC traces obtained from oocytes expressing NR1/NR2A(trunC) NMDARs (B) or NR1/NR2A(delC) NMDARs (C). (D) Histogram showing the mean potentiation of glutamate-evoked currents by EDTA. No significant differences in the levels of potentiation were observed between each of the three NR2A constructs.

with the extracellular binding site for polyamines (Williams *et al*., 1994; Zhang *et al*., 1994), since it only occurs in NMDARs containing the NR1-1a (exon 5-lacking) NMDAR subunit splice variant and is absent in receptors expressing the NR1-1b (exon 5-containing) NMDAR subunit splice variant. While the NR1-1a splice variant was also used in our study and the potentiation, like that of the Paoletti *et al*. (1995) study, occurred at saturating glutamate/glycine concentration, it differs in that the potentiation we observed occurred at NR2A-containing NMDARs and at negative holding potentials. It remains to be determined whether there are similarities between the Mg^{2+} potentiation of NR2B-containing NMDARs (Paoletti *et al*., 1995) and the potentiation we have seen with NR2A(delC)-containing NMDARs. Further experiments using the NR1-1b NMDAR subunit together with NR2B NMDAR subunits with mutated CTDs, as well as determining the extent of potentiation at positive holding potentials are required to characterize further this action of low concentrations of Mg^{2+}. Nevertheless, since this potentiating effect of Mg^{2+} is only seen at low concentrations it is unlikely to compromise any interpretation of studies that have investigated CTD-mutant NR2A NMDAR subunits (which have used solutions where Mg^{2+} levels are generally $\geq$1 mmol·L^{-1}). Memantine, like Mg^{2+}, is a channel blocker of NMDARs, albeit that it exhibits less voltage dependence (e.g. see Wrighton *et al*., 2008) although there is some overlap in the sites to which memantine and Mg^{2+} exert their blocking effects. Unlike with Mg^{2+}, however, no potentiation of NR1/NR2A(delC) NMDAR-mediated currents was observed with memantine and indeed the levels of inhibition seen at the three voltages studied with the range of memantine concentrations used were similar for each of the three NMDAR combinations we investigated.

The NR2A NMDAR subunit contains many phosphorylation sites (e.g. see Trinidad *et al*., 2008), and phosphorylation of three tyrosine residues in the CTD of NR2A NMDAR subunits by the tyrosine kinase Src relieves high affinity inhibition by Zn^{2+} (Zheng *et al*., 1998). We postulated that there might be some differences in the extent of the block, at each of the NMDAR constructs, by the contaminant levels of low concentrations of Zn^{2+} present in our external recording solutions. However, the EDTA-induced potentiation of receptors containing either NR2A(WT), NR2A(trunC) or NR2A(delC) NMDAR subunits was similar. This indicates that while phosphorylation of residues in the CTD results in 'long-range' communication between an intracellularly located and an extracellularly located domain, there does not appear to be a 'tonic' interaction between these domains in the absence of Src phosphorylation. Protein–protein interactions at the CTD may also influence these properties, as intracellular CTD associated proteins such as PSD-95 have been shown to reduce Zn^{2+} inhibition and

eliminate Src dependent potentiation of NMDAR currents (Yamada *et al.*, 2002).

Conclusion

It is recognized that NMDARs contain four 'functional domains' which determine in a semi-autonomous manner pharmacological properties concerning by way of example: modulation by pH, polyamines, Zn^{2+} (the ATD), agonist and (competitive) antagonist binding (the LBD), ion permeation and block (membrane-associated domains) and interactions with scaffolding and intracellular signalling complexes (the CTD). Nevertheless, critical interactions between these domains also exist and this prompted us to investigate in our study whether the CTD could influence certain pharmacological properties of NMDARs. Our data show that of the parameters we studied there were only minor influences of the CTD – there was a small increase in glycine potency and an intriguing potentiation by low concentrations of Mg^{2+} of responses mediated by NMDARs lacking the NR2A CTD. However, these small effects are unlikely to compromise interpretation of studies that make use of CTD-mutated recombinant receptors or transgenic mice in investigations of the role of the CTD in NMDAR signalling.

Acknowledgements

This work was supported by funds from the Undergraduate Neuroscience Honours Programme at the University of Edinburgh. RS was supported by The Wellcome Trust.

Conflict of interest

The authors state no conflict of interest.

References

Alexander SPH, Mathie A, Peters JA (2008). Guide to Receptors and Channels (GRAC), 3rd edn. *Br J Pharmacol* **153** (Suppl. 2): S1–S209.

Burnashev N, Schoepfer R, Monyer H, Ruppersberg JP, Gunter W, Seeburg PH *et al.* (1992). Control by asparagine residues of calcium permeability and magnesium blockade in the NMDA receptor. *Science* **257**: 1415–1419.

Chen HSV, Lipton SA (2005). Pharmacological implications of two distinct mechanisms of interaction of memantine with *N*-methyl-D-aspartate-gated channels. *J Pharmacol Exp Ther* **314**: 961–971.

Chen PE, Wyllie DJA (2006). Pharmacological insights obtained from structure-function studies of ionotropic glutamate receptors. *Br J Pharmacol* **147**: 839–853.

Chen PE, Geballe MT, Stansfeld PJ, Johnston AR, Yuan H, Jacob AL *et al.* (2005). Structural features of the glutamate binding site in recombinant NR1/NR2A *N*-methyl-D-aspartate receptors determined by site-directed mutagenesis and molecular modeling. *Mol Pharmacol* **67**: 1470–1484.

Chen PE, Geballe MT, Katz E, Erreger K, Livesey M, O'Toole KK *et al.* (2008). Modulation of glycine potency in rat recombinant NMDA receptors containing chimeric NR2A/2D subunits expressed in *Xenopus laevis* oocytes. *J Physiol* **586**: 227–245.

Cull-Candy S, Brickley S, Farrant M (2001). NMDA receptor subunits: diversity, development and disease. *Curr Opin Neurobiol* **11**: 327–335.

Dingledine R, Borges K, Bowie D, Traynelis SF (1999). The glutamate receptor ion channels. *Pharmacol Rev* **51**: 7–61.

Dravid SM, Erreger K, Yuan H, Nicholson K, Le P, Lyuboslavsky P *et al.* (2007). Subunit-specific mechanisms and proton sensitivity of NMDA receptor channel block. *J Physiol* **581**: 107–128.

Erreger K, Chen PE, Wyllie DJA, Traynelis SF (2004). Glutamate receptor gating. *Crit Rev Neurobiol* **16**: 187–224.

Erreger K, Geballe MT, Kristensen A, Chen PE, Hansen KB, Lee CJ *et al.* (2007). Subunit-specific agonist activity at NR2A-, NR2B-, NR2C-, and NR2D-containing *N*-methyl-D-aspartate glutamate receptors. *Mol Pharmacol* **72**: 907–920.

Frizelle PA, Chen PE, Wyllie DJA (2006). Equilibrium constants for (*R*)-[(*S*)-1-(4-bromo-phenyl)-ethylamino]-(2,3-dioxo-1,2,3,4-tetrahydroquinoxalin-5-yl)-methyl]-phosphonic acid (NVP-AAM077) acting at recombinant NR1/NR2A and NR1/NR2B NMDA receptors: implications for studies of synaptic transmission. *Mol Pharmacol* **70**: 1022–1032.

Furukawa H, Singh SK, Mancusso R, Gouaux E (2005). Subunit arrangement and function in NMDA receptors. *Nature* **438**: 185–192.

Gardoni F, Bellone C, Cattabeni F, Di Luca M (2001). Protein kinase C activation modulates alpha-calmodulin kinase II binding to NR2A subunit of *N*-methyl-D-aspartate receptor complex. *J Biol Chem* **276**: 7609–7613.

Garry EM, Moss A, Delaney A, O'Neill F, Blakemore J, Bowen J *et al.* (2003). Neuropathic sensitization of behavioral reflexes and spinal NMDA receptor/CaM Kinase interactions are disrupted in PSD-95 mutant mice. *Curr Biol* **13**: 321–328.

Hawkins LM, Prybylowski K, Chang K, Moussan C, Stephenson FA, Wenthold RJ (2004). Export from the endoplasmic reticulum of assembled *N*-methyl-D-aspartic acid receptors is controlled by a motif in the C terminus of the NR2 subunit. *J Biol Chem* **279**: 28903–28910.

Iwamoto T, Yamada Y, Hori K, Watanabe Y, Sobue K, Inui M (2004). Differential modulation of NR1-NR2A and NR1-NR2B subtypes of NMDA receptor by PDZ domain-containing proteins. *J Neurochem* **89**: 100–108.

Kornau HC, Schenker LT, Kennedy MB, Seeburg PH (1995). Domain interaction between NMDA receptor subunits and the postsynaptic density protein PSD-95. *Science* **269**: 1737–1740.

Kuner T, Schoepfer R (1996). Multiple structural elements determine subunit specificity of Mg^{2+} block in NMDA receptor channels. *J Neurosci* **16**: 3549–3558.

Lin Y, Skeberdis VA, Francesconi A, Bennett MV, Zukin RS (2004). Postsynaptic density protein-95 regulates NMDA channel gating and surface expression. *J Neurosci* **24**: 10138–10148.

Lin Y, Jover-Mengual T, Wong J, Bennett MV, Zukin RS (2006). PSD-95 and PKC converge in regulating NMDA receptor trafficking and gating. *Proc Natl Acad Sci USA* **103**: 19902–19907.

Mayer ML, Westbrook GL, Guthrie PB (1984). Voltage-dependent block by Mg^{2+} of NMDA responses in spinal cord neurons. *Nature* **309**: 261–263.

Migaud M, Charlesworth P, Dempster M, Webster LC, Watabe AM, Makhinson M *et al.* (1998). Enhanced long-term potentiation and impaired learning in mice with mutant postsynaptic density-95 protein. *Nature* **396**: 433–439.

Monyer H, Sprengel R, Schoepfer R, Herb A, Higuchi M, Lomeli H *et al.* (1992). Heteromeric NMDA receptors: molecular and functional distinction of subtypes. *Science* **256**: 1217–1221.

Monyer H, Burnashev N, Laurie DJ, Sakmann B, Seeburg PH (1994). Developmental and regional expression in the rat brain and functional properties of four NMDA receptors. *Neuron* **12**: 529–540.

Nowak L, Bregestovski P, Ascher P, Herbet A, Prochiantz A (1984).

Magnesium gates glutamate-activated channels in mouse central neurons. *Nature* **307**: 462–465.

Paoletti P, Neyton J, Ascher P (1995). Glycine-independent and subunit-specific potentiation of NMDA responses by extracellular Mg^{2+}. *Neuron* **15**: 1109–1120.

Paoletti P, Ascher P, Neyton J (1997). High-affinity zinc inhibition of NMDA NR1-NR2A receptors. *J Neurosci* **17**: 5711–5725.

Parsons CG, Danysz W, Bartmann A, Spielmanns P, Frankiewicz T, Hesselink M *et al*. (1999). Amino-alkyl-cyclohexanes are novel uncompetitive NMDA receptor antagonists with strong voltage-dependency and fast blocking kinetics: *in vitro* and *in vivo* characterization. *Neuropharmacology* **38**: 85–108.

Rossi P, Sola E, Taglietti V, Borchardt T, Steigerwald F, Utvik JK *et al*. (2002). NMDA Receptor 2 (NR2) C-terminal control of NR open probability regulates synaptic transmission and plasticity at a cerebellar synapse. *J Neurosci* **22**: 9687–9697.

Rutter AR, Stephenson FA (2000). Coexpression of Postsynaptic Density-95 protein with NMDA receptors results in enhanced receptor expression together with a decreased sensitivity to L-glutamate. *J Neurochem* **75**: 2501–2510.

Rutter AR, Freeman FM, Stephenson FA (2002). Further characterization of the molecular interaction between PSD-95 and NMDA receptors: the effect of the NR1 splice variant and evidence for modulation of channel gating. *J Neurochem* **81**: 1298–1307.

Ryan TJ, Emes RD, Grant SG, Komiyama NH (2008). Evolution of NMDA receptor cytoplasmic interaction domains: implications for organisation of synaptic signalling complexes. *BMC Neurosci* **9**: 6.

Sprengel R, Suchanek B, Amico C, Brusa R, Burnashev N, Rozov A *et al*. (1998). Importance of the intracellular domain of NR2 subunits for NMDA receptor function *in vivo*. *Cell* **92**: 279–289.

Steigerwald F, Schulz TW, Schenker LT, Kennedy MB, Seeburg PH, Kohr G (2000). C-terminal truncation of NR2A subunits impairs synaptic but not extrasynaptic localization of NMDA receptors. *J Neurosci* **20**: 4573–4581.

Traynelis SF, Burgess MF, Zheng F, Lyuboslavsky P, Powers JL (1998). Control of voltage-independent zinc inhibition of NMDA receptors by the NR1 subunit. *J Neurosci* **18**: 6163–6175.

Trinidad JC, Thalhammer A, Specht CG, Lynn AJ, Baker PR, Schoepfer R *et al*. (2008). Quantitative analysis of synaptic phosphorylation and protein expression. *Mol Cell Proteomics* **7**: 684–696.

Wang LY, MacDonald JF (1995). Modulation by magnesium of the affinity of NMDA receptors for glycine in murine hippocampal neurones. *J Physiol* **486**: 83–95.

Williams K, Zappia AM, Pritchett DB, Shen YM, Molinoff PB (1994). Sensitivity of the *N*-methyl-D-aspartate receptor to polyamines is controlled by NR2 subunits. *Mol Pharmacol* **45**: 803–809.

Wollmuth LP, Kuner T, Sakmann B (1998). Adjacent asparagines in the NR2-subunit of the NMDA receptor channel control the voltage-dependent block by extracellular Mg^{2+}. *J Physiol* **506**: 13–32.

Wrighton DC, Baker EJ, Chen PE, Wyllie DJA (2008). Mg^{2+} and memantine block of rat recombinant NMDA receptors containing chimeric NR2A/2D subunits expressed in *Xenopus laevis* oocytes. *J Physiol* **586**: 211–225.

Wyllie DJA, Chen PE (2007). Taking the time to study competitive antagonism. *Br J Pharmacol* **150**: 541–551.

Yamada Y, Chochi Y, Takamiya K, Sobue K, Inui M (1999). Modulation of the channel activity of the epsilon2/zeta1-subtype *N*-methyl-D-aspartate receptor by PSD-95. *J Biol Chem* **274**: 6647–6652.

Yamada Y, Iwamoto T, Watanabe Y, Sobue K, Inui M (2002). PSD-95 eliminates Src-induced potentiation of NR1/NR2A-subtype NMDA receptor channels and reduces high-affinity zinc inhibition. *J Neurochem* **81**: 758–764.

Zhang L, Zheng X, Paupard M, Wang AP, Santchi L, Friedman LK *et al*. (1994). Spermine potentiation of recombinant *N*-methyl-D-aspartate receptors is affected by subunit composition. *Proc Natl Acad Sci USA* **91**: 10883–10887.

Zheng F, Gingrich MB, Traynelis SF, Conn PJ (1998). Tyrosine kinase potentiates NMDA receptor currents by reducing tonic zinc inhibition. *Nat Neurosci* **1**: 185–191.